Hogan S, Wiberg PL, Reidenbach MA (2021) Utilizing airborne LiDAR data to quantify marsh edge morphology and the role of oyster reefs in mitigating marsh erosion. Mar Ecol Prog Ser 669:17-31. https://doi.org/10.3354/meps13728

Utilizing airborne LiDAR data to quantify marsh edge morphology and the role of oyster reefs in mitigating marsh erosion

Sara Hogan[1*], Patricia Wiberg[1], Matthew Reidenbach[1]

[1]Department of Environmental Sciences, University of Virginia, Charlottesville, Virginia, USA 22904

ABSTRACT

We develop methods to quantify marsh edge morphology using airborne LiDAR data and validate these methods with in-situ observations. We then apply these methods within the context of oyster reef restoration within the shallow coastal bays of Virginia, USA by comparing retreat and morphology quantified at paired reef-lined and control marsh edges at ten different marsh sites. Retreat metrics were analyzed between 2002 and 2015, utilizing a LiDAR derived edge for the year 2015 from points of maximum slope and aerial imagery pre-2015. Retreat was also compared before and after oyster reef restoration to determine if reefs slow erosion. We found that slope statistics from airborne LiDAR elevation data can accurately capture marsh edge morphology. Retreat rate, measured at edges typically found near the vegetation line, was not significantly different between reef-lined and control marshes and ranged from 0.14 to 0.79 m yr^{-1}. Both retreat rate (ρ = -0.90) and net movement (ρ = -0.88) were strongly correlated to marsh edge elevation. Exposed control marshes had significantly greater mean and maximum slope values compared to reef-lined marshes. The mean edge slope for exposed marshes was 11.4º and for reef-lined marshes was 6.0º. We hypothesize that oyster reefs are causing an elongation of the marsh edge by reducing retreat at lower elevations of the marsh edge. Therefore, changes in marsh edge morphology may be a precursor to changes in marsh retreat

*sh8kj@virginia.edu

rates over longer timescales and emphasizes the need for repeated LiDAR measurements to capture processes driving marsh edge dynamics.

Keywords: marsh edge, morphology, LIDAR, oyster reefs, retreat

1. INTRODUCTION

1.1. Remote sensing of marshes

Conservatively, 1-2% of marshes are lost per year (Duarte et al. 2008), with loss accelerating over the last two centuries (Davidson 2014). Although it has been found that marshes may be able to keep pace with sea level rise in the vertical dimension (Blum et al. 2020), marsh edge erosion in the lateral dimension reduces areal marsh platform habitat (Kirwan et al. 2010, Mariotti & Fagherazzi 2013). For marshes found along coastal bays, lateral migration that is associated with eroding edges has been recorded at rates greater than 1 m yr^{-1} (Kastler & Wiberg 1996, Day et al. 1998, McLoughlin et al. 2015). These rates are likely affected by edge morphology, where different erosional processes are responsible for transporting sediment (Van de Koppel et al. 2005, Leonardi et al. 2016a).

To determine marsh edge characteristics and their rates of change, it is necessary to have an accurate means for measuring and monitoring spatial morphology. Remote sensing is increasingly being utilized for topographic analyses of marshes and proves advantageous over other surveying techniques by providing a method for non-invasive data collection that also produces robust, accurate datasets (Schenk & Csatho 2002). Specifically, the creation of digital elevation models (DEMs) through Light Detecting and Ranging (LiDAR) surveys has been useful for characterizing marshes at broader scales than surface elevation tables and erosion markers can capture (Mattheus et al. 2010). Other derivatives of elevation, such as slope, aspect, and curvature, have been fundamental in remotely sensing the characteristics of various landscapes (Glenn et al. 2006). Because change in ocean shorelines using LiDAR has been largely successful (Stockdon et al. 2002), this technology is likely to be useful in analyzing marsh edges as well. While previous studies have largely relied on aerial imagery to capture horizontal change in marsh edge location (e.g. Kastler & Wiberg 1996, McLoughlin et al. 2015, Leonardi et al. 2016a), this imagery cannot readily provide information about marsh edge elevation and steepness. LiDAR elevation mapping of salt marshes has been largely successful at classifying vegetation types (Morris et al. 2005, Hladik et al. 2013) and geomorphic features (Millette et al. 2010, Chassereau et al. 2011, Chirol et al. 2018), although there can be elevation errors in regions of dense vegetation owing to reduced laser penetration (Schmid et al. 2011, Medieros et al. 2015). LiDAR has also been used to monitor marsh edge retreat and volumetric accretion rates (Mattheus et al. 2010, Zhao et al. 2017). However, few studies have utilized remote sensing to describe marsh margins compared to those describing platform elevations and vegetation (Goodwin & Mudd 2020). Within marsh margin studies, both in-situ and remote sensing methods have been developed to locate marsh edges based on elevation and slope measurements (Goodwin et al. 2018, Farris et al. 2019, Goodwin & Mudd 2020). Goodwin and Mudd (2020) showed that airborne LiDAR data with a resolution of 1 m^2 can be used to adequately locate marsh margins in macrotidal settings. With repeated measures, detailed quantification of erosional processes such as those accomplished for other coastal shorelines (White & Wang 2003, Obu et al. 2017) are likely feasible for marsh edges. However, the utility of LiDAR-based topographic analysis of marsh edge morphology and retreat rates in microtidal systems remains to be verified.

1.2. Marsh edge processes

Marsh edge morphologies vary widely ranging from sharp cliff faces to gently sloping edges (Allen 2000, Tonelli et al. 2010, McLoughlin et al. 2015). The different morphologies are largely influenced by the local erosional processes taking place. These processes are dependent on tidal water level relative to platform elevation because it affects where and how tidal and wave energy is received. Elevation can dictate if breaking wave action is more important in defining edge morphology than bottom stresses caused by frictional drag over adjacent tidal flats (Tonelli et al. 2010, Francalanci et al. 2013). Three different erosional processes have been described in shaping marsh edge morphology in shallow coastal environments, including those found along the mid-Atlantic region of the USA (McLoughlin 2010, Priestas et al. 2015). The first process is undercutting and toppling. This occurs when sediment is more quickly eroded from the lower layers of substrate resulting in a platform overhang, which eventually bends and topples creating sharp, vertical scarps (Schwimmer 2001, Tonelli et al. 2010, Francalanci et al. 2013). This occurs most often where sediment is sandy and less cohesive. Secondly, root scalping occurs when waves break at elevations similar to the platform and weak areas in the vegetation mat detach, leaving the underlying sediment susceptible to erosion (Priestas et al. 2015). This can lead to a terrace or step-like marsh edge morphology. Lastly, bioerosion influences morphology where burrowing organisms are present in sufficient densities to weaken sediment causing cracks that widen and lead to block detachment (Schwimmer 2001) and sharp scarps. Marsh edges characterized by undercutting or crack formation are likely to be more prone to failure and rapid retreat, compared to terraced or gently sloping marsh edges where flow-generated bottom shear stresses entrain sediment at a slower rate (Francalanci et al. 2013).

1.3. Marsh edge and oyster reef coupling

Often found near marsh edges, oyster reefs are thought to behave as a coupled dynamical system with adjacent marshes (McGlathery et al. 2011). Therefore, the presence of oyster reefs, and the hard, stable substrate they form, may be a crucial component shaping marsh edge characteristics. Oysters reefs themselves can have different morphologies depending on the tidal-driven current and wave environment (Bahrs & Lanier 1981, Lenihan 1999), including those running either parallel or perpendicular to shorelines (fringe reefs) as wells as, irregular mounds found further from shore (patch reefs). These differences can be important because it is well established that oyster reefs can change the hydrodynamic energy in estuarine environments by increasing drag on the flow (Dame & Patten 1981, Whitman & Reidenbach 2012, Volaric et al. 2020) and attenuating wave energy (Chowdhury et al. 2019, Wiberg et al. 2019). Concurrently, oyster reefs also stabilize estuarine sediments by reducing resuspension and encouraging deposition of fine particles (Meyer et al. 1997, Reidenbach et al. 2013, Colden et al. 2016,). Combined, these environmental alterations suggest that oyster reefs can help mitigate marsh edge erosion. Erosion rates measured at marsh edges along the south and east coasts of the United States have shown that oyster reefs, especially in low wave energy environments, can have mitigative effects on erosion (Meyer et al. 1997, Piazza et al. 2005). Because oysters within Virginia’s coastal bays are primarily intertidal (Hogan & Reidenbach 2019), the ability of oyster reefs to alter both the local mean flow (Volaric et al. 2018) and wave energy (Wiberg et al. 2019) varies as water depth changes due to tides. Wave dissipation is most effective when water depth over the reefs is relatively shallow (Chowdhury 2019, Wiberg et al. 2019).

1.4. Study Objectives

The goal of this study is to first develop a general methodology using airborne LiDAR elevation data to accurately locate and characterize marsh edges bordering coastal bays in a microtidal environment using slope statistics. We then apply these methods to investigate if there are observable differences in marsh edge retreat and morphology at marshes both exposed to open water and those located behind natural and restored oyster reefs. To examine whether retreat is affected by oyster reef restoration, we build on a dataset of digitized shorelines from aerial imagery for mainland marshes from 2002 and 2009 (McLoughlin et al. 2013) and compare these to LiDAR collected in 2015 to analyze retreat for various marsh edges within Virginia, U.S.A. coastal bays. We quantify rate of retreat for reef-lined and control locations and rate of retreat before and after reef construction. Additionally, we compare marsh edge morphology for these same sites using the derived slope statistics. We then use the data to determine what relationships exist between marsh edge morphology and the physical environment to determine factors that can make marshes more vulnerable to retreat.

2. Materials & Methods

2.1. Study Site

The marshes and oyster reefs considered in this study are located within the Virginia Coast Reserve (VCR) on the eastern side of the Delmarva Peninsula, Virginia, USA. The VCR is a National Science Foundation Long-term Ecological Research (LTER) site encompassing over 100 km of coastline and coastal bays (Figure 1). The VCR contains many diverse coastal habitats including salt marshes, oyster reefs, and mudflats. Oysters in the VCR are of the species *Crassostrea virginica* and found largely in the intertidal zone. The coastal bays experience a mean tidal range of approximately 1.2 m with limited freshwater input (Marotti & Fagherazzi 2013). Narrow inlets through barrier islands connect the bays to the Atlantic Ocean and create a gradient of flushing and water residences times (Safak et al. 2015). Winds are dominantly from the north-northeast direction in winter and from the south in summer (Wiberg et al. 2019) and wave-driven erosion has been found to be the primary driver of marsh migration within these shallow coastal bays (Tonelli et al. 2010, Mariotti & Fagherazzi 2013, Leonardi et al. 2016b). Wave energy impacting the marsh edge depends on a combination of water depth, fetch distance, wind direction, and drag imposed along the seafloor (Fagherazzi & Wiberg 2009).

2.2. Method development: LiDAR-based classification of marsh edges

A USGS airborne LiDAR dataset covering the extent of the VCR was collected in 2015 (Dewberry 2016) and was used to classify land area and locate marsh edges. The LiDAR elevation dataset was converted into a raster with pixel dimensions of 0.76 m x 0.76 m and projected in WGS84 UTM Zone 18 and vertical datum NAVD88. It has 95% confidence values for vertical accuracy of 12.5 cm for non-vegetated and 17.7 cm for vegetated terrain (Dewberry 2016). Each surveying flight was conducted within two hours of low tide, however, some intertidal features were still underwater and were assigned (i.e., hydroflattened) to the level of the water surface elevation. From preliminary investigation of the LiDAR elevations, we found that the LiDAR survey captured the transition of many marsh platforms into surrounding mudflats, making identification of marsh edge location and morphology possible.

To determine if marsh edge morphology and retreat are affected by adjacency to oyster reefs, ten different marsh edges with fringing oyster reefs or adjacent to patch oyster reefs (within approximately 20 m of visible land) were chosen for investigation, referred to as reef-lined marshes (Table 1, Figure 1). For each site, we paired the reef-lined marsh with a nearby control marsh without an adjacent reef but having the same shoreline orientation. Edges varied in length between approximately 100 to 300 m. A point and shapefile dataset provided by The Nature Conservancy was used to locate areas of restored reefs with known build dates. The reefs include a combination of fringe and patch reefs restored using either deposited oyster or whelk shell. Build dates span from 2003 – 2019, forming 62 reefs covering a total of 51.8 acres. Two additional reef locations (Site 6 and Site 7, Table 1) from a 2008 NOAA funded survey of oyster reefs (Ross & Luckenbach 2009) were included to supplement the restored reef data. Patches within 40 m of a marsh edge were included in reef acreage for these two locations (Table 1). Many of these patch reefs are now considered 'reference' or 'natural' because of their decades old age, though all reefs in the region have been impacted by human activity and they were likely restored in some capacity through protective efforts. Additional details on edges and associated reefs are found in Table 1. Only reefs restored prior to 2015, when LiDAR elevation data was acquired, were included in this analysis. Restored reefs allowed us to place a date on the reefs and test for their ability to provide coastal protection. For each pair of edges, a marsh edge was first digitized where the scarp was visible on the elevation layer at resolution 1:1000. Approximately the same length of edge was digitized for both control and reef-lined marshes at each site, although length varied by site to conform to oyster coverage.

Marsh surface slope was calculated using the 3D Analyst Slope tool in ArcMap 10.5 after removal of hydroflattened elevations which were identified locally as pixels with a constant minimum low elevation extending to the bay. The tool employs the average maximum technique with 8 neighbors around a center cell to find the maximum rate of elevation change, where the expression:

$$\text{slope degrees} = \left(\tan^{-1}\sqrt{\frac{dz}{dx}^2 + \frac{dz}{dy}^2}\right) * \frac{180}{\pi}$$

is used to calculate the degree of slope at each pixel using data from the 8 neighboring pixels.

At each marsh, we used the Linear Sampling toolbox added to ArcMap 10.5 to cast perpendicular transects 5 m apart extending 10 m in each direction from the digitized edge and extracted terrain slope data every meter along each transect. For each transect, we found the point of maximum slope, and used that as a proxy for the marsh edge in 2015 (Figure 2). The mean of these values was calculated to give an average edge slope for each marsh.

Additionally, a 10 m buffer was created around each edge and slope data was extracted to determine the mean slope in the buffer area around the edge using the zonal statistics tool (Figure 2). Zonal statistics extract the data from each pixel within a given polygon to calculate statistics for an area. This can be useful to describe marsh edges that are more ramped, or terraced, and not well described by just a single edge location. It also allows for a repeatable method of determining slope at each marsh. These 10 m buffer locations are referred to as ‘buffer areas’.

To validate the utility of using airborne LiDAR for characterizing marsh edge morphology in a microtidal system, we compared remotely-sensed marsh elevation and edge descriptions with measured in-situ data obtained in 2010 (McLoughlin 2010). The in-situ edge surveys were obtained with a Trimble R8 GNSS System for 5 edges at 4 different marshes located within Hog Island Bay, Virginia. We recreated elevation profiles extending from the mudflat into the marsh platform for multiple transects at each marsh edge and compared the modeled and in-situ elevation profiles and morphologic descriptions with extracted slope statistics. Although there was a time difference of 5 years between datasets, the use of a stable marsh edge and marsh platforms allowed for comparisons to be made.

2.3. Quantifying marsh edge retreat and morphology occurring at reef-lined and control marshes

2.3.1. Marsh site selection and physical environments

We compared the elevations between reef-lined marsh and control marsh locations at each site to determine if the two marshes were well paired and determine the drivers of retreat and morphology by extracting elevation to 10 m buffer areas (See 2.2). Elevations are reported in meters NAVD88. Platform elevation, taken to be the mean of the maximum point of elevation along transects spaced every 5 m along the digitized edge, and marsh edge elevation, the elevation at the point of maximum slope along transects, were analyzed (See 2.2, Figure 2).

Wave exposure along the marsh edge was estimated using the local fetch distance. Fetch was previously modeled for the VCR in ArcMap 9.2 using scripts from USGS (Kremer & Reidenbach 2020). Mean fetch for summer 2015 was made into a raster grid of 30 x 30 m pixels, after being weighted by the proportion of time wind came from each direction. Direction was based on 10^{o} increments and wind data came from the Wachapreague NOAA station (Kremer & Reidenbach 2020). Fetch data was extracted to each buffer area and the mean value was used to represent each location. Where the previously modeled fetch dataset did not cover the entire buffer area, the average of the partial data was used. In cases where there was no data present, the average of the 3 values nearest the approximate ends and midpoint of the digitized edge were averaged, each within 50 m of the digitized edge.

2.3.2. Marsh retreat

For the five mainland marsh sites (Sites 2, 3, 4, 6, & 7, Figure 1), we quantified changes in marsh edge position between the years 2002, 2009, and 2015. These dates were chosen because mainland marshes were previously digitized in the VCR for years 2002 and 2009 from aerial imagery (McLoughlin et al. 2015) and LiDAR was taken in 2015. To compute the marsh edge for 2015 we connected the points of maximum slope (see 2.2) along transects at each marsh. The points were manually inspected and edited to account for edge effect discrepancies. To determine marsh retreat, shorelines and baselines edited in ArcGIS ArcMap 10.5 were imported to R. We used digitized shorelines for years 2002, 2009, and 2015. The Analyzing

Boundary Movement Using R (AMBUR) package in R was used to assess marsh edge movement (Jackson et al. 2012). Transects were drawn every 5 m and filtered using a moving window of 5 transects along the length of each marsh (Jackson et al. 2012). The intersections of transects with shorelines were used to calculate and analyze end point rate (EPR m yr^{-1}), which is the rate of shoreline change between the youngest and oldest shorelines, and net change in shoreline movement (NC m) between the years 2002 and 2015. We used a 2-way ANOVA to explain the difference in mean retreat values from 2002 – 2015 with factors including type of marsh edge (reef-lined or control) and site ($\alpha = 0.05$). We also analyzed the rate of retreat before (2002-2009) and after (2009-2015) reef restoration using percent change in EPR and NC. The percent change analysis between time periods was completed where mainland adjacent reefs had known restoration dates after 2009 (Sites 2, 3, & 4). Again, two-way ANOVAs were used with percent change in EPR and NC as dependent variables and marsh type and site as independent variables.

2.3.3. Marsh edge morphology

We used the 10 m radius buffer at each marsh to capture the edge topography for all 10 sites. As previously described (Section 2.2), slope statistics were calculated using zonal statistics. Using the transect method (described in Section 2.2), the points representing the slope-defined edge were found and averaged to find the mean edge slope for each marsh. A 2-way ANOVA was used to determine if marsh edge morphology for the buffer area mean slope and mean edge slope were explained by type of marsh (reef-lined or control) and site. To validate the use of a 10 m radius buffer search area, the slope data was compared with results from a smaller, 5 m radius buffer region. We found that although values differed slightly, the same patterns for reef-lined and control marshes were observed for mean, standard deviation, and CV of slope for 5 m and 10 m buffer areas. We used the 10 m buffer areas for analysis because they offer a more complete picture of the marsh and mudflat system.

2.2.4. Drivers of marsh edge retreat and morphology

Spearman's rank correlations were used to examine possible relationships between EPR, NC, and physical (mean fetch, mean platform elevation, and mean edge elevation) and slope variables because of the non-normal distribution of the retreat data. We also analyzed whether mean edge slope and buffer area mean slope, our metrics for marsh edge morphology, were correlated with the physical variables for each location (n = 10). Pearson's correlation methods were used for the normally distributed, continuous variables with one mean value for each location (n = 20).

3. RESULTS

3.1. Method development: LiDAR-based quantification of marsh edges

Remotely-sensed airborne LiDAR elevations were strongly correlated with in-situ GPS elevation data ($r^2 = 0.92$, n = 114, Figure A1). Overall, we found that LiDAR and in-situ elevation profiles agreed for the stable marsh and marsh platforms (Figure A2). The comparison of profiles from in-situ (2010) and LiDAR (2015) surveys captures the lateral retreat that occurred in 5 years' time. We found the highest buffer area mean slope and edge slopes at the scarped edge marshes and the lowest values at the ramped marsh (Table A1, Figure A3).

3.2. Marsh retreat and morphology occurring at reef-lined and control marsh edges

3.2.1. Marsh edge retreat

Results for shoreline movement suggested considerable variability in EPR (end point rate m yr^{-1}) and NC (net change m) across the sites for the period from 2002 to 2015 with values ranging from (mean ± se) -0.79 ± 0.07 to -0.14 ± 0.01 m yr^{-1} and -10.05 ± 0.84 to -1.74 ± 0.17 m, respectively (Table 2, Figure 4, Figure 5). The results of the 2-way ANOVAs suggested that there was no significant difference in retreat for reef-lined and control marsh edges for mean EPR ($p = 0.91$) and mean NC ($p = 0.91$) from 2002 – 2015 (Figure 5). However, there were significant differences in mean EPR ($p < 0.01$) and mean NC ($p < 0.01$) with site, where site 4, Brownsville, experienced significantly greater retreat compared to other sites.

There was no statistically significant difference in percent change of retreat variables for the time periods 2002-2009 and 2009-2015 with marsh type or site for both EPR ($p = 0.7$, $p = 0.5$) and NC ($p = 0.7$, $p = 0.5$) (Table 3). No clear patterns were found in change in retreat for reef-lined and control marshes at these sites. Contrary to our hypothesis, the greatest percent reduction in retreat rate (EPR) and movement (NC) was observed at a control marsh, Site 2B.

3.2.3. Marsh edge morphology

Marsh edges without adjacent oyster reefs (control locations) had a greater buffer area mean slope ($p= 0.005$), indicating steeper topographies, compared to reef-lined marshes (Figure 6). The mean buffer area slope for reef-lined marshes was 2.5º, while that for control marshes was 3.7º. There was no significant difference in mean slope with site ($p = 0.07$). Similar results were found for edge slope, where control locations had significantly higher edge slope values ($p=0.01$), compared to reef-lined marsh locations (Figure 6), but no significant difference with site ($p = 0.5$). The mean edge slope for control marsh locations was 11.4º, while the mean for reef-lined marsh locations was 6.0º. The greatest difference, 15.6º, was observed at Site 1, and the smallest was less than 1º at Site 2. Slope statistics (Figure 6) largely correspond with marsh edge elevation data (Figure 3A), where control marshes have higher elevations and slope values, except for Site 7, where the pattern is reversed, and the higher reef-lined edge also has higher slope values.

3.2.4. Regression and correlation analyses

The physical data extracted from each marsh edge, including buffer area elevation, edge elevation, platform elevation, and mean fetch, are shown in Figure 3. While there is variation between sites, the reef-lined and control edges at each site often have similar values. We also found that for reef-lined locations the marsh platform was found to be higher than the affronting reefs. Relative to NAVD88 mean platform elevation was 0.07 m, mean reef crest was -0.69 m, and the mean difference between the platform elevation and reef crests was 0.76 m. Correlation analyses between retreat and explanatory variables for the 5 sites (n = 10, marsh and control edges) suggest that marsh edge elevation was the only variable significantly correlated with retreat variables. There were strong significant negative correlations for EPR ($\rho = -0.90$, $p < 0.001$) and NC ($\rho = -0.88$, $p < 0.01$) with the elevation of the marsh edge (Table 4). The negative correlation corresponds to an increase in onshore movement of the marsh edge with increased marsh edge elevation. Mean fetch (EPR $p = 0.13$, NC $p = 0.14$) and mean platform elevation (EPR $p = 0.14$, NC $p = 0.13$, Table 4) both showed negative, but not significant, relationships.

The only significant correlations between physical and slope variables were with platform elevation (Table 4). Buffer area mean slope showed a significant positive correlation with mean platform elevation ($\rho = 0.65$, $p < 0.01$) and non-significant correlations with mean edge elevation ($\rho = 0.12$, $p = 0.67$), and mean fetch distance ($\rho = 0.07$, $p = 0.77$). Similar results were found for correlations with mean marsh edge slope. There was a significant positive correlation with mean platform elevation ($\rho = 0.76$, $p < 0.001$), a moderate though non-significant positive correlation with mean edge elevation (ρ =0.35, p = 0.13), and almost no correlation with mean fetch (ρ = 0.01, p=0.98). This indicates that marshes with more highly elevated platforms are more likely to have greater sloping edges.

For both EPR and NC, there was very low correlation to marsh edge slope (ρ = 0.07 and ρ = 0.05, respectively) and buffer area mean slope (ρ = 0.44 and ρ = 0.42).

4. DISCUSSION

4.1. Drivers of Morphology and Retreat

We developed and validated a technique using remotely-sensed elevation to quantify marsh edge morphology and retreat that can be used to monitor change with repeated measures. The LiDAR dataset used to characterize slope yielded a wide range of slope values, with edge slopes ranging from 2.6^{0} to 26.0^{0} and buffer area mean slopes ranging from 1.5^{0} to 11^{0}. A methodology using remotely-sensed elevation data can capture the morphology of large sections of the marsh edge more quickly and easily than in-situ measurements.

We found that higher marsh edges were correlated with greater rate of retreat (EPR) and net change (NC) and that marsh edges are likely to be more steeply sloping if they have high platforms. These correlations support that marsh edge erosion is driven by wave action and previous findings that highly elevated platforms are more likely to be undercut and experience greater edge erosion compared to more gently sloping morphologies (Schwimmer 2001, Moller & Spencer 2002, McLoughlin 2015). The importance of platform elevation is also highlighted by studies that suggest marsh elevation and tide level can affect the energy driving erosion of the marsh edge since wave thrust is significantly decreased when a marsh is submerged, but otherwise increased as water becomes deeper owing to the larger waves that can develop (Tonelli et al. 2010, Wiberg et al. 2019).

While our findings support the important role of marsh edge and platform elevation on marsh retreat and edge morphology, the correlations were made with only 10 and 20 sections of marsh edge, for retreat and morphology, respectively. The majority of reefs fronting the reef-lined edges were restored reefs, which may reflect an effect of decision-making by managers to restore reefs in front of lower elevated marshes that may be less likely to erode, presenting a potential factor in reef placement. Oysters may also preferentially grow along low elevation edges, helping to explain why we found reef-lined edges at lower elevations with corresponding lower slope values, except at one site (Site 7). At that site, the reef-lined edge was more highly elevated and had higher slope values, consistent with marsh edge elevation being the most important predictor of marsh slope. Platform elevation was also significantly, though less strongly, correlated with mean slope and edge slope (0.65 and 0.76 respectively; Table 4). These relationships among physical and retreat variables suggest that highly elevated marsh edges are most susceptible to retreat and should be targeted by coastal managers when trying to identify vulnerable shorelines. While there was not a significant relationship between retreat and marsh edge slope variables, this data was limited by the number of sites available from LiDAR data matched with restored reefs, and time between reef construction and data acquisition. Increasing the scale of the investigation with repeated LiDAR measurements and the addition of more sites may yield more clarifying results.

4.2. Morphology and retreat applied to oyster presence

Our results indicate that the presence of oyster reefs affects marsh edge morphology, with reef-lined marshes having more gently sloping edges compared to marsh edges lacking an adjacent reef. We did not find significant correlations between mean fetch distance and marsh morphology and retreat. Although there was no significant difference between reef-lined and control marshes for retreat variables, retreat rates ranged from 0.14 to 0.79 m yr^{-1} over the years 2002 – 2015 (Table 2) and were similar to past observations within Virginia's coastal bays and the Mid-Atlantic region (Schwimmer 2001, Taube 2013, McLoughlin et al. 2015). McLoughlin et al. (2015) and Taube (2013) both studied marshes within the VCR using shorelines from imagery from 1957 to 2009. McLoughlin et al. (2015) surveyed marshes at 4 sites bordering a large coastal bay; 3 of 4 had rates of erosion near or greater than 1 m yr^{-1} (0.98 – 1.63 m yr^{-1}). Taube (2013), who focused on mainland-bordering marshes, found 5 of 8 marshes to be retreating between 0.15 and 0.27 m yr^{-1}, one extreme location retreating at 1.58 m yr^{-1}, and 2 prograding marshes (0.46 and -0.0004 m yr^{-1}). Our rates of retreat more closely correspond to the findings from Taube (2013), who also observed marshes retreating both in the presence and absence of oyster reefs.

The marsh edges derived using the locations of maximum slope found from LiDAR data largely agreed with the edges digitized from aerial imagery for the years 2002 and 2009 (McLoughlin 2013). Therefore, it is likely that the points of maximum slope are also closely defining the vegetation line at the marsh edge. This is also observed when manually inspecting the edges drawn from maximum slope locations. The data shows that the mean slope of the edge and buffer area slope are lower for reef-lined marshes, but no significant difference is found in retreat along the upper elevations of the marsh edge nearer the vegetation line and platform. We hypothesize that this is because erosion along the subtidal toe of the marsh edge, which is at an elevation similar to the reefs (Hogan & Reidenbach 2019), is reduced due to the presence of oyster reefs while the rate of retreat of the intertidal marsh edge is relatively unchanged by the presence of reefs. From this, we can hypothesize that reefs cause the marsh edges to elongate by stretching the marsh edge transition from the platform towards the lower intertidal zone, thereby causing the morphology to become less steep. Over time, oyster presence may begin to influence erosion rates along the upper marsh edge near the vegetation line due to increased frictional wave dissipation and/or other physical factors, such as advancing vegetation, along the elongated marsh edge. Our data are too limited to test this hypothesis and repeated LiDAR measurements over multiple years to decades may be necessary to capture these changes occurring at marsh edges due to the presence of oyster reefs.

4.3. Limitations of data extracted from LiDAR

The elevation and derived slope data used to compare morphology and create the marsh edges are dependent on the resolution and accuracy of the LiDAR measurements. While rasterized LiDAR elevation data on the order of 1 m^2 has been reported to satisfactorily describe edges (Goodwin & Mudd 2020), the resolution of the data limits the accuracy of derived calculations. Elevation data can be distorted over highly sloped terrain because values of elevation can change dramatically over short distances (Hodgson & Bresnahan 2004) and therefore more accurate estimates of slope, and often higher values, are found with reduced cell size (Grohmann 2015). The error associated with derived slope is also proportional to resolution and for high-resolution DEMs, error from slope algorithms is less important than error derived from the data (Zhou & Liu 2004). Determining error propagation is possible by using raw LiDAR data and plotting root mean square errors (RMSE), but also requires knowledge of spatial dependencies and autocorrelations (Hunter & Goodchild 1997).

Our analysis used slope data calculated using a pixel size of 0.76 m in each dimension and a moving kernel of 9 cells. The resulting slope values were therefore smoothed over this spatial dimension. Although, the agreement between the in-situ GPS and LiDAR data shows variability at the point level as is expected from the published vertical accuracy (12.5 and 17 cm for non-vegetated and vegetated terrain, respectively), the overall agreement was very high ($r^2 = 0.92$, Figure A1) and we are confident in the quality of the elevation data used in the slope calculations. Since paired marshes are located close to one another, the accuracy in slope measurements is likely similar between paired sites, enabling us to understand how slope statistics compare between different locations, even if the slope values themselves are minorly affected by data and algorithm error.

4.4. Conclusions

In conclusion, the marsh edge morphology and retreat values we extracted from airborne LiDAR data supports that reef-lined marsh edges are more gently sloping compared to exposed marshes and the change in morphology is likely a precursor to measurable change in retreat. The elevation of the marsh edge was significantly correlated to retreat, while platform elevation was significantly correlated to marsh slope. The methods presented here can be utilized for monitoring future changes in marsh edge movement and morphology if repeated LiDAR surveys are conducted. Additionally, our findings can be used to locate areas vulnerable to change to aid in coastal management and conservation efforts. However, an integrated assessment of how vegetation dynamics (van de Koppel et al. 2005, Faegin et al. 2009, Feagin et al. 2009, Francalanci et al. 2013) and invertebrate behavior (Escapa et al. 2007, Davidson & Rivera 2010) affect marshes and marsh edge dynamics may be necessary to create a more holistic understanding of marsh retreat and morphology.

5. ACKNOWLEDGEMENTS

In addition to support from within the Department of Environmental Sciences at the University of Virginia, we would like to thank the Nature Conservancy working within the Virginia Coast Reserve for sharing resources and local knowledge and researchers and staff at the Anheuser-Busch Coastal Research Center. This research was funded by the National Science Foundation grant DEB-1832221 to the Virginia Coast Reserve Long Term Ecological Research project. M. Reidenbach was supported by NSF grant OCE-1151314.

6. LITERATURE CITED

Allen JRL (2000) Morphodynamics of Holocene salt marshes: a review sketch from the Atlantic and Southern North Sea coasts of Europe. Quat Sci Rev, 19 (12): 1155-1231

Bahr LM, Lanier WP (1981) The ecology of intertidal oyster reefs of the South Atlantic coast: a community profile. FWS/OBS-81/15. US Fish and Wildlife Service, Office of Biological Services, Washington, DC

Blum LK, Christian RR, Wiberg PL, Cahoon DR (2020) Processes influencing elevation and high marsh conversion to low marsh in a temperate saltmarsh. Estuar Coasts doi.org/10.1007/s12237-020-00796-z

Chassereau JE, Bell JM, Torres R (2011) A comparison of GPS and lidar salt marsh DEMs. Earth Surf Process Landf 36: 1770-1775

Chirol C, Haigh ID, Pontee N, Thompson CE, Gallop SL (2018) Parametrizing tidal creek morphology in mature saltmarshes using semi-automated extraction from lidar. Remote Sens Environ 209: 291-311

Chowdhury MSN, Walles B, Sharifuzzman SM, Hossain MS, Ysebaert T, Smaal AC (2019) Oyster breakwater reefs promote adjacent mudflat stability and salt marsh growth in a monsoon dominated subtropical coast. Sci Rep 9,8549 https://doi.org/10.1038/s41598-019-44925-6

Colden A, Fall KA, Massey GM, Friedrichs C (2016) Sediment suspension and deposition across restored oyster reefs of varying orientation to flow: implications for restoration. Estuar Coasts 39(5): 1435 –1448

Dame RF, Patten BC (1981) Analysis of energy flows in an intertidal oyster reef. Mar Eco Prog Ser 5:115-124

Davidson NC (2014) How much wetland has the world lost? Long-term and recent trends in global wetland area. Mar Freshw Res 65: 934-941

Davidson TM, Rivera CE (2010) Accelerated erosion of saltmarshes infested by the non-native burrowing crustacean *Sphaeroma quoianum*. Mar Eco Prog Ser 419: 129-136

Day JW, Scarton F, Rismondo A, Are D (1998) Rapid deterioration of a salt marsh in Venice Lagoon, Italy. J Coast Res 14(2): 583 – 590

Dewberry (2016) Eastern shore Virginia QL2 LiDAR BAA. USGS task order G15PD00284

Duarte CM, Dennison WC, Orth RJW, Carruthers TJB (2008) The charisma of coastal ecosystems: addressing the imbalance. Estuar Coasts: J CERF 31:233-238

Escapa M, Minkoff DR, Perillo GME, Iribarne O (2007) Direct and indirect effects of burrowing crab *Chasmagnathus granulatus* activities on erosion of southwest Atlantic *Sarcocornia*-dominated marshes. Limnol and Oceanogr 52(6) 2340-2349F

Fagherazzi S, Wiberg, PL (2009) Importance of wind conditions, fetch, and water levels on wave-generated shear stresses in shallow intertidal basins. J Geophys Res 114:12pp

Farris AS, Defne Z, Ganju NK (2019) Identifying salt marsh shorelines from remotely sensed elevation data and imagery. Remote Sens 11: 1795-1812

Feagin RA, Lozada-Bernard SM, Ravens TM, Moller I, Yeager KM, Baird AH (2009) Does vegetation prevent wave erosion of salt marsh edges? Proc Nat Acad of Sci 106(25): 10109-10113

Francalanci S, Bendoni M, Rinaldi M, Solari L (2013) Ecomorphodynamic evolution of salt marshes: Experimental observations of bank retreat processes. Geomorphology 195: 53-65

Glenn NF, Streutker DR, Chadwick DJ, Thackray GD, Dorsch SJ (2006) Analysis of LiDAR-derived topographic information for characterizing and differentiating landslide morphology and activity. Geomorphology 73(102) 131-148

Goodwin, GCH, Mudd SM, Clubb FJ. 2018. Unsupervised detection of salt marsh platforms: a topographic method. Earth Surf Dynam 6:239-255

Goodwin CH, Mudd SM (2020) Detecting the morphology of prograding and retreating marsh margins- example of a mega-tidal bay. Remote Sens 12: 13- 39

Grohmann CH (2015) Effects of spatial resolution on slope and aspect derivation for regional-scale analysis. Comput Geosci 77: 111-117 DOI:10.1016/j.cageo.2015.02.003

Hladik C, Schalles J, Alber M (2013) Salt marsh elevation and habitat mapping using hyperspectral and LIDAR data. Remote Sens Environ 139: 318-330

Hodgson ME, Bresnahan P (2004) Accuracy of airborne Lidar-derived elevation: empirical assessment and error budget. Photogramm Eng Remote Sensing 70: 331 – 339

Hogan S, Reidenbach MA (2019) Quantifying and analyzing intertidal oyster reefs utilizing LiDAR-based remote sensing. Marine Ecol Prog Ser 630: 83-99

Hunter GJ, Goodchild MF (1997) Modeling the uncertainty of slope and aspect derived from spatial databases. Geogr Anal 29(1): 35-49

Jackson Jr. CW, Alexander CR, Bush DM (2012) Application of the AMBUR R package for spatio-temporal analysis of shoreline change: Jekyll Island, Georgia, USA. Comput Geosci 41: 199-207

Kastler JA, Wiberg PL (1996) Sedimentation and boundary changes of Virginia salt marshes. Estuar Coast Shelf Sci 42: 683-700

Kirwan ML, Guntenspergen GR, D'Alpaos A, Morris JT, Mudd SM, Temmerman S (2010) Limits on the adaptability of coastal marshes to rising sea level. Geophys Res Lett 37, L23401 doi:10.1029/2010GL045489

Kremer M, Reidenbach MA (2020) Modeled wind fetch for the bays of the Virginia Coast Reserve. Virginia Coast Reserve Long-Term Ecological Research Project Data Publication knb-lter-vcr.300.1 doi:doi:10.6073/pasta/6e0e574063bf500ef5f2d855126697e6

Lenihan HS (1999) Physical-biological coupling on oyster reefs: how habitat structure influences individual performance. Ecol Monogr 69: 251−275

Leonardi N, Defne Z, Ganju NK, Fagherazzi S (2016) Salt marsh erosion rates and boundary features in a shallow bay. J Geophys Res Earth Surf 121: 1861 -1875

Leonardi N, Ganju NK, Fagherazzi S (2016) A linear relationship between wave power and erosion determines salt-marsh resilience to violent storms and hurricanes. Pro Nat Acad Sci USA 113: 64-8

Mariotti G, Fagherazzi S (2013) Critical width of tidal flats triggers marsh collapse in the absence of sea-level rise. Proc Nat Acad Sci USA 110:5353-5356

Mattheus CR, Rodriguez AB, McKee BA, Currin CA (2010) Impact of land-use change and hard structures on the evolution of fringing marsh shorelines. Estuar Coast Shelf Sci 88: 365-376.

McGlathery KJ, Reidenbach MA, D'Odorico PAOLO, Fagherazzi S, Pace ML, Porter JH (2013) Nonlinear dynamics and alternative stable states in shallow coastal systems. Oceanogr 26: 220-231

McLoughlin, SM (2010) Erosional processes along salt marshes edges on the Eastern Shore of Virginia. Master's thesis, University of Virginia, Charlottesville, VA

McLoughlin SM, McGlathery KJ, Wiberg PL (2013) Quantifying changes along mainland marshes in the Virginia Coast Reserve, 1957 – 2011: GIS data. Virginia Coast Reserve Long-Term Ecological Research Project Data Publication knb-lter-vcr.196.12 doi:10.6073/pasta/e2115c3f1fce44522b4c3ded4ae19a79

McLoughlin SM, Wiberg PL, Safak I, McGLathery KJ (2015) Rates and forcing of marsh edge erosion in a shallow coastal bay. Estuar and Coasts 38: 620-638

Medeiros S, Hagen S, Weishampel J, Angelo J (2015) Adjusting Lidar-derived digital terrain models in coastal models based on estimated aboveground biomass density. Remote Sensing 7: 3507 – 3525

Meyer DL, Townsend EC, Thayer GW (1997) Stabilization and erosion control value of oyster cultch for intertidal marsh. Restor Ecol 5: 93-99

Millette TL, Argow BA, Marcano E, Hayward C, Hopkinson CS, Valentine V (2010) Salt marsh geomorphological analyses via integration of multitemporal multispectral remote sensing with LiDAR and GIS. J Coast Res 26: 809 -816

Moller I, Spencer T (2002) Wave dissipation over macro-tidal saltmarshes: effects of marsh edge typology and vegetation change. J Coast Res SI 36: 506-521

Morris JT, Porter D, Neet M, Nobel PA, Schmidt L (2005) Integrating LIDAR elevation data, multi-spectral imagery and neural network modelling for marsh characterization. Int J Remote Sens 26: 5221-5234

Piazza EP, Banks PD, La Peyre MK (2005) The potential for created oyster shell reefs as a sustainable shoreline protection strategy in Louisiana. Restor Ecol 13: 499-506

Priestas AM, Mariotti G, Leonardi N, Fagherazzi S (2015) Coupled wave energy and erosion dynamics along a salt marsh boundary, Hog Island Bay, Virginia, USA. J Mar Sci Eng 3: 1041-1065

Reidenbach MA, Berg P, Hume A, Hansen JCR, Whitman ER (2013) Hydrodynamics of intertidal oyster reefs: The influence of boundary layer flow processes on sediment and oxygen exchange. Limnol Oceanogr Fluids Environ 3: 225 -239

Ross PG, Luckenbach MW (2009) Population assessment of eastern oysters (Crassostrea virginica) in the seaside coastal bays. Virginia Coastal Zone Management Program, Virginia Department of Environmental Quality, Richmond Virginia

Safak I, Wiberg PL, Kurum MO, Richardson DL (2015) Controls on residence time and exchange in a system of shallow coastal bays. Cont Shelf Res 97: 7-20

Schenk T, Csatho B (2002) Fusion of LiDAR data and aerial imagery for a more complete surface description. Int Arch Photogramm Remote Sens 97: 7 – 20

Schmid KA, Hadley BC, Wijekoon N (2011) Vertical accuracy and use of topographic LiDAR data in coastal marshes. J Coast Res 27:116-132

Schwimmer, RA (2001) Rates and processes of marsh shoreline erosion in Rehoboth Bay, Delaware, USA. J Coast Res 17: 672 -683

Southwell MW, Veenstra JJ, Adams CD, Scarlett EV, Payne KB. 2017. Changes in sediment characteristics upon oyster reef restoration, NE Florida, USA. J Coast Zone Manag 20(1) DOI: 10.4172/2473-3350.1000442

Stockdon HF, Sallenger Jr AH, List JH, Holman RA (2002) Estimation of shoreline position and change using airborne topographic Lidar data. J Coast Res 18(3): 502-513

Taube SR (2013) Impacts of fringing oyster reefs on wave attenuation and marsh erosion rates. Master's Thesis, University of Virginia, Charlottesville, VA

Tonelli M, Fagherazzi S, Petti M (2010) Modeling wave impact on salt marsh boundaries. J Geophs Res 115: C09028

Van de Koppel J, van der Wal D, Bakker JP, Herman PMJ (2005) Self-organization and vegetation collapse in salt marsh ecosystems. Am Nat 165(1): E1 – E12

Volaric M.P., Berg P., and Reidenbach M.A., 2018, Oxygen metabolism of intertidal oyster reefs measured by aquatic eddy covariance, *Marine Ecology Progress Series*, 599, 75-91

Volaric M.P., Berg P., and Reidenbach M.A., 2020, Drivers of oyster reef ecosystem metabolism measured across multiple timescales, *Estuaries and Coasts*, doi:10.1007/s12237-020-00745-w.

White SA, Wang Y (2003) Utilizing DEMs derived from LIDAR data to analyze morphologic change in the North Carolina coastline. Remote Sens Environ 85: 39 – 47

Whitman ER, Reidenbach MA (2012) Benthic flow environments affect recruitment of *Crassostrea virginica* larvae to an intertidal oyster reef. Mar Eco Prog Ser 463: 117-191

Wiberg PL, Taube SR, Ferguson AE, Kremer MR, Reidenbach MA (2019) Wave attenuation by oyster reefs in shallow coastal bays. Estuar and Coast 42: 331-347

Zhao Y, Wang Q, Wang D, Wang YP (2017) Rapid formation of marsh-edge cliffs, Jiangsu coast, China. Mar Geol 385:260-273

Zhou Q, Liu X (2004) Analysis of errors of derived slope and aspect related to DEM data properties. Comput Geosci 30: 369-378

7. TABLES

Table 1. Metadata for the paired locations including site, marsh type (A = reef-lined, B = control), local reef name, edge length, type of restoration, shape, year restored, acres of reef (N/A 'not applicable' describes control sites where there are no reefs present, therefore no acreage), pixel count, the mean and standard deviation of slope extracted to each buffer area, and for reef-lined marshes the mean reef crest elevation relative to NAVD8 and local mean sea level (lmsl). For patch reefs surveyed 2008, the acreage represents the area of reefs within 40 m from the digitized edge.

Site	**Marsh Type**	**Local reef name**	**Edge Length (m)**	**Type**	**Shape**	**Year**	**Acreage**	**Pixel Count**	**Mean**	**Std**	**Reef elevation (m NAVD88/ m lmsl)**
1	A	Black Rock	175	shell	fringe	2010	0.88	5800	2.34	1.82	-1.0 /-0.91
1	B		175	control	control	N/A	N/A	5964	4.11	5.74	
2	A	Boxtree1	115	whelk	fringe	2012	0.55	2818	4.10	3.26	-0.98/-0.89
2	B		115	control	control	N/A	N/A	2998	5.25	3.15	
3	A	Boxtree2	120	whelk	fringe	2012	0.54	3388	3.90	3.02	-0.88/-0.77
3	B		120	control	control	N/A	N/A	3634	4.17	3.23	
4	A	Brownsville	180	shell	fringe	2010	0.73	5225	3.24	2.42	-0.53/-0.44
4	B		180	control	control	N/A	N/A	4892	3.76	3.41	
5	A	Cob	290	shell	fringe	2005	1.62	7500	1.64	0.97	-0.55/-0.44
5	B		290	control	control	N/A	N/a	9946	2.23	1.89	
6	A	Fowling Point	225	natural	patch	Before 2008	0.76	7607	2.23	1.82	-0.44/-0.34
6	B		225	control	control	N/A	N/A	7538	3.71	1.89	
7	A	Hillcrest	170	natural	patch	Before 2008	2.5	6109	2.31	1.69	-0.71/-0.67
7	B		170	control	control	N/A	N/A	6392	1.75	1.02	

8	A	Outlet	150	shell	patch	2008	0.78	6090	1.46	0.70	-0.46/-0.36
8	B		150	control	control	N/A	N/A	5356	3.37	3.25	
9	A	Paramore	175	shell	fringe	2008	1.04	6144	1.60	1.128	-0.91/-0.82
				shell	patch	2010	2.58				
9	B		175	control	control	N/A	N/A	4649	4.62	4.023	
10	A	Point of rocks	200	shell	patch	2010	0.97	7474	2.12	1.76	-0.47/-0.36
10	B		200	control	control	N/A	N/A	7484	3.81	3.56	

Table 2. EPR (m yr^{-1}) and NC (m) and standard error (SE) for each marsh from 2002-2015 where marsh type A = reef-lined and B = control.

Site	**Marsh Type**	**Local reef name**	**EPR (m yr^{-1}) 2002-2015**	**EPR (m yr^{-1}) SE**	**NC (m) 2002-2015**	**NC (m) SE**
2	A	Boxtree1	-0.26	0.02	-3.27	0.25
2	B		-0.14	0.01	-1.74	0.17
3	A	Boxtree2	-0.26	0.03	-3.26	0.34
3	B		-0.22	0.04	-2.84	0.45
4	A	Brownsville	-0.74	0.07	-9.4	0.85
4	B		-0.79	0.07	-10.05	0.84
6	A	Fowling Point	-0.29	0.08	-3.58	1.03
6	B		-0.42	0.05	-5.35	0.64
7	A	Hillcrest	-0.28	0.03	-3.62	0.4
7	B		-0.24	0.05	-3.01	0.62

Table 3. Change and percent change from the periods 2002-2009 and 2009-2015 for end point rate (EPR m yr^{-1}) and net change (NC m) of movement. White fill indicates reduced shoreward movement, while grey indicates increased shoreward movement between the two time periods, where marsh type A = reef-lined and B = control.

Site	Marsh Type	Local Reef Name	EPR (m yr^{-1}) 2002-2009	EPR (m yr^{-1}) 2009-2015	EPR Δ	EPR % Δ	NC (m) 2002-2009	NC (m) 2009-2015	NC Δ	NC % Δ
2	A	Boxtree1	-0.27	-0.24	0.03	-12.5	-1.89	-1.38	0.51	-36.96
2	B		-0.21	-0.05	0.16	-320	-1.45	-0.29	1.16	-400
3	A	Boxtree2	-0.34	-0.15	0.19	-126.67	-2.41	-0.85	1.56	-183.53
3	B		0	-0.49	-0.49	100	0	-2.84	-2.84	100
4	A	Brownsville	-0.6	-0.9	-0.3	33.33	-4.22	-5.17	-0.95	18.38
4	B		0.04	-1.93	-1.97	102.07	0.28	-10.33	-10.61	102.71

Table 4. Correlation tests performed between retreat (EPR and NC) and marsh edge slope values with physical variables. Spearman's correlation tests were performed with non-normal retreat variables, and Pearson's correlations performed with marsh slope variables.

Retreat Variable	Explanatory variable	Correlation estimate	P-value
EPR	Fetch	-0.51	0.13
	Platform elevation	-0.50	0.14
	Edge elevation	-0.90	< 0.001
	Edge slope	0.07	0.84
	Mean slope	0.44	0.21
NC	Fetch	-0.50	0.14
	Platform elevation	-0.52	0.13
	Edge elevation	-0.88	< 0.01
	Edge slope	0.05	0.89
	Mean slope	0.42	0.23
Buffer area mean slope	Fetch	0.07	0.77
	Platform elevation	0.65	< 0.01
	Edge elevation	0.12	0.67
Edge slope	Fetch	0.01	0.98
	Platform elevation	0.76	< 0.001
	Edge elevation	0.35	0.13

8. FIGURES

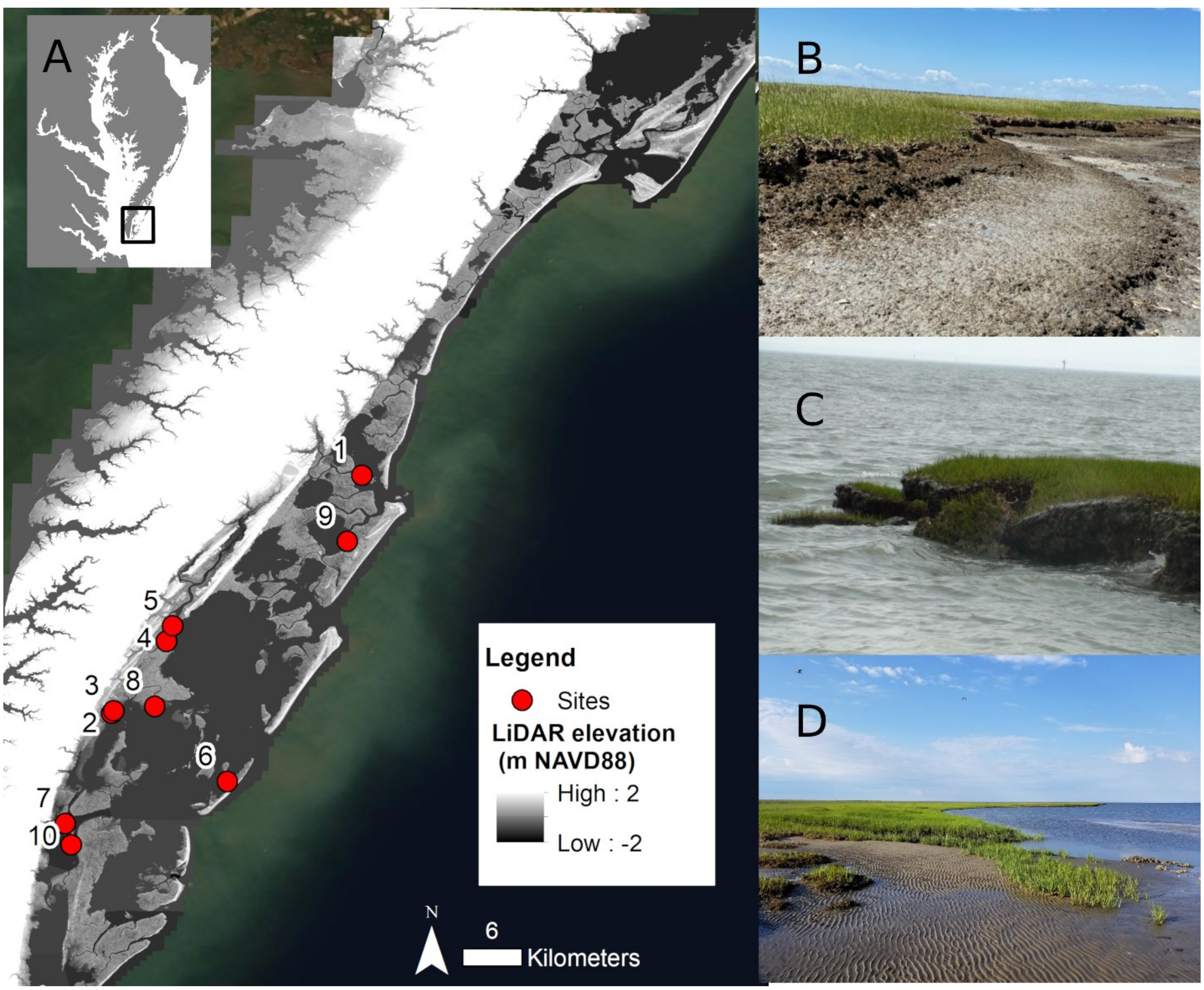
A
B
C
D
1
9
5
4
3
8
2
6
7
10
Legend
Sites
LiDAR elevation
(m NAVD88)
High : 2
Low : -2
N
6
Kilometers

Figure 1. A) Marsh sites located in the Virginia Coast Reserve. At each site both a control and reef-lined marsh edge were located for analysis. On the right, examples of marshes with B) terraced, C) scarped, and D) ramped morphologies found in the VCR are shown. Photo credit for C & D: Qingguang Zhu, UVA

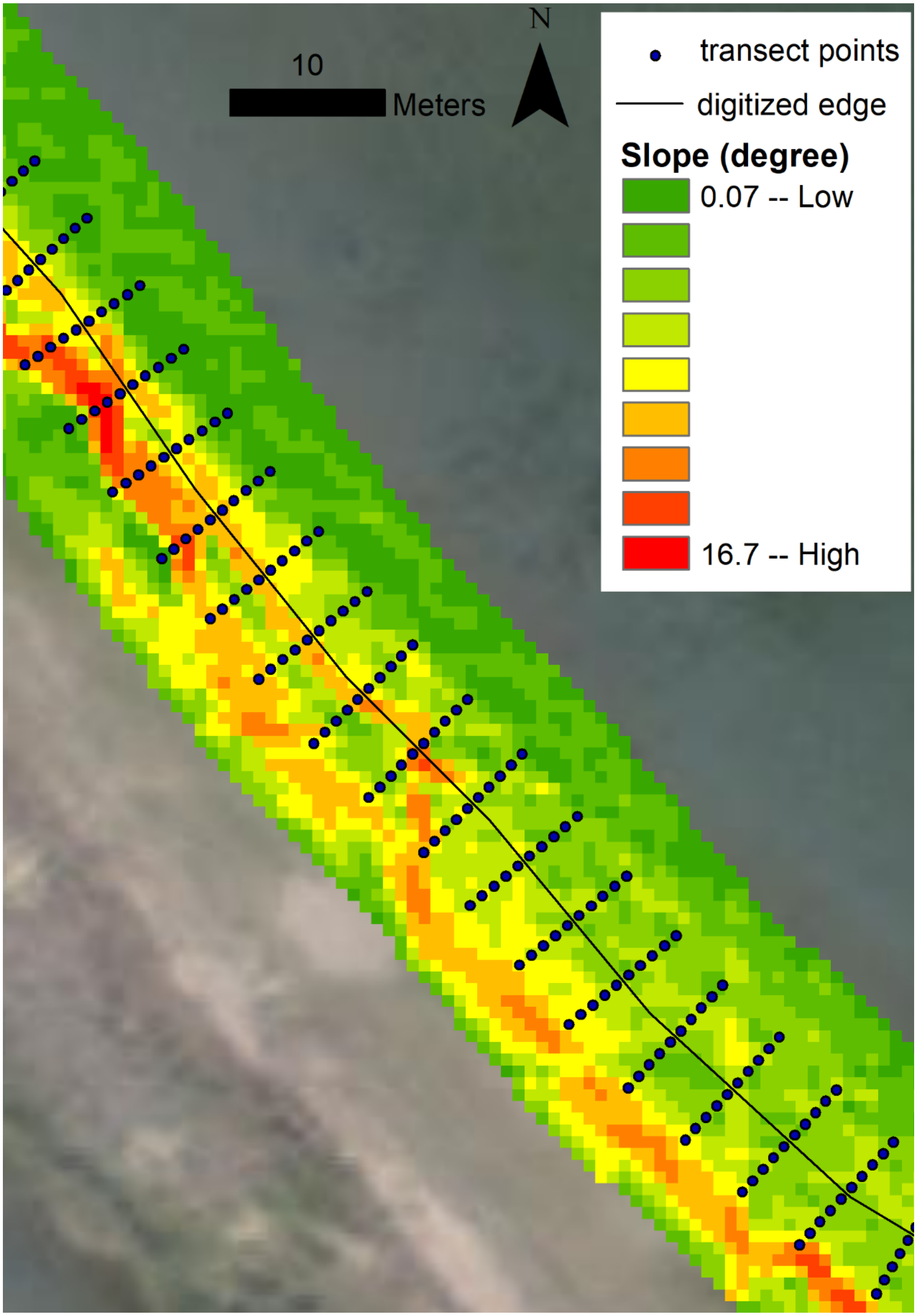
10
Meters
N
transect points
digitized edge
Slope (degree)
0.07 -- Low
16.7 -- High

1

Figure 2. Slope data within the buffer area region for site 6B, a control marsh edge. Low to high values of slope (degree) and shown from green to red. The in-situ surveyed edge is shown in black, with perpendicular transects cast every 5 m with points every 1 m where slope data was extracted to locate the marsh edge.

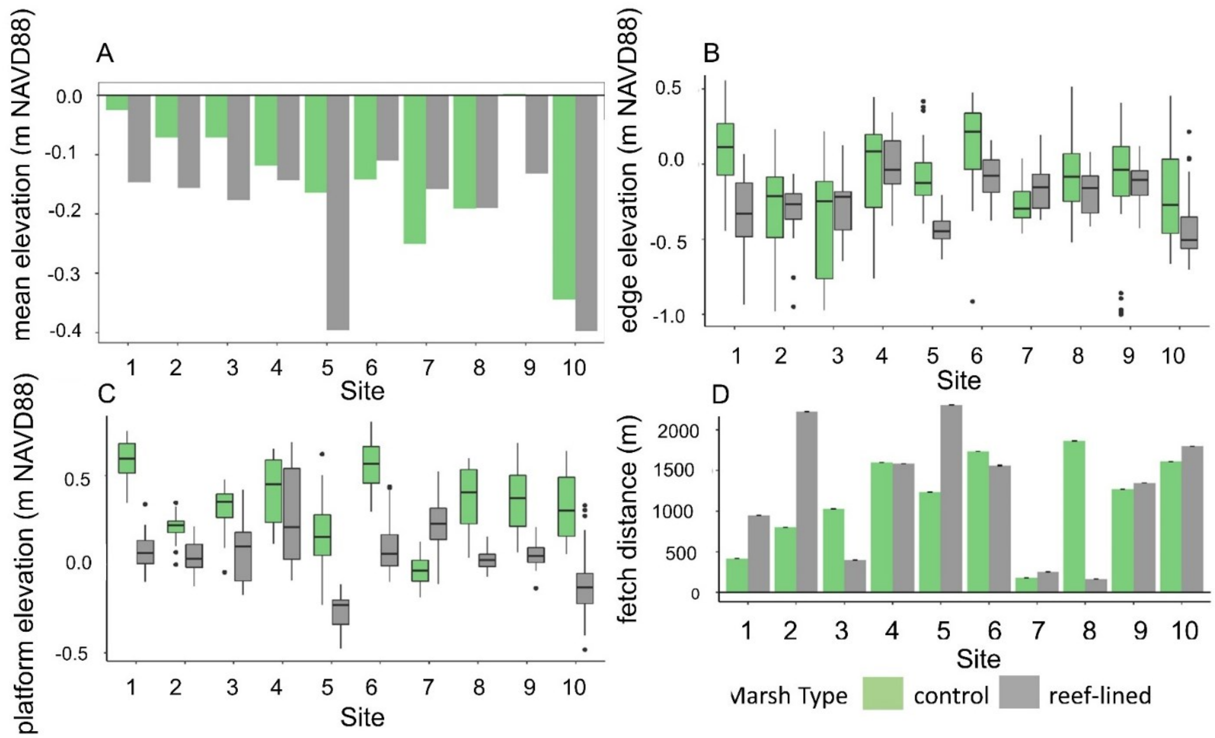

Figure 3. Physical characteristics for each marsh including: A) Mean elevation within the buffer areas at each marsh edge B) boxplot of edge elevations from transects at each site C) boxplot of platform elevations from transects at each site D) mean fetch distance (m). Elevations are measured in m NAVD88. Grey bars indicate reef-lined marshes and green bars indicate control marshes at each site. For boxplots: boxes indicate the interquartile range (IQR) with the interior line representing the median, whiskers the maximum and minimum (up to 1.5 times the IQR range), and dots represent outliers beyond the range.

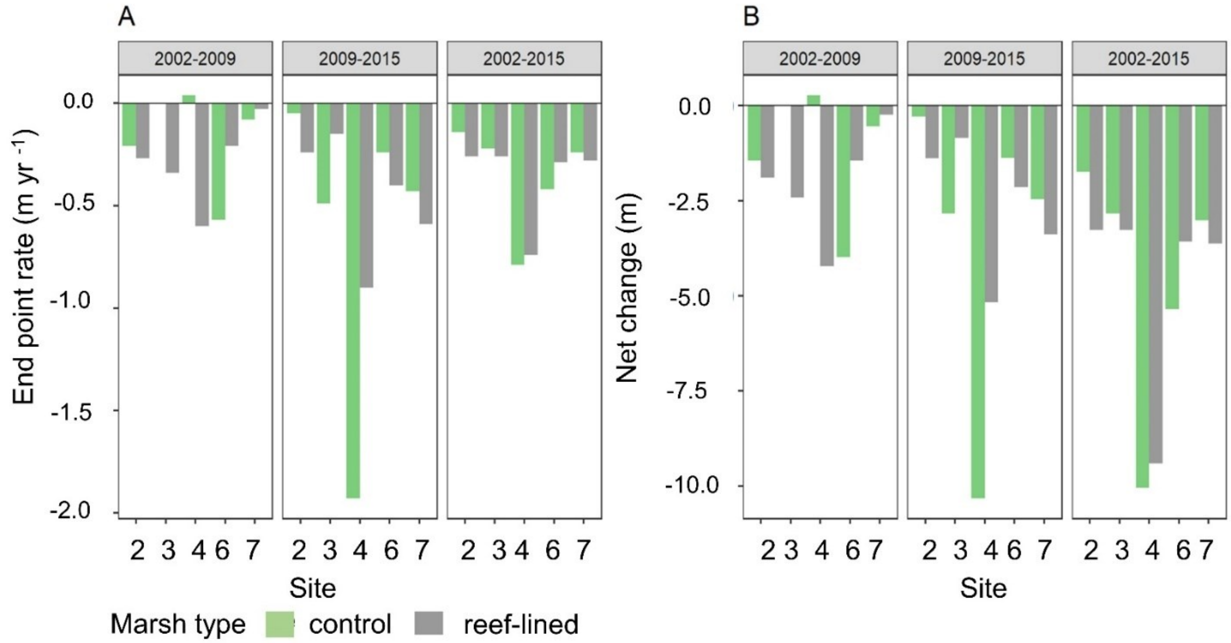

Figure 4. Mean EPR (A) and NC (B) at each location for each time period. Grey bars indicate reef-lined marshes and green bars indicate control marshes at each site.

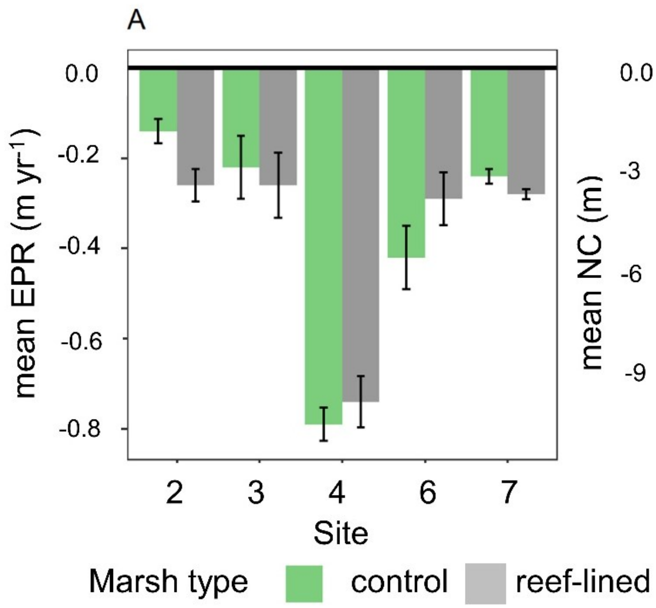

Figure 5. A) Mean EPR and B) NC with standard error bars for paired marshes at each site between 2002 – 2015. Grey bars indicate reef-lined marshes and green bars indicate control marshes at each site.

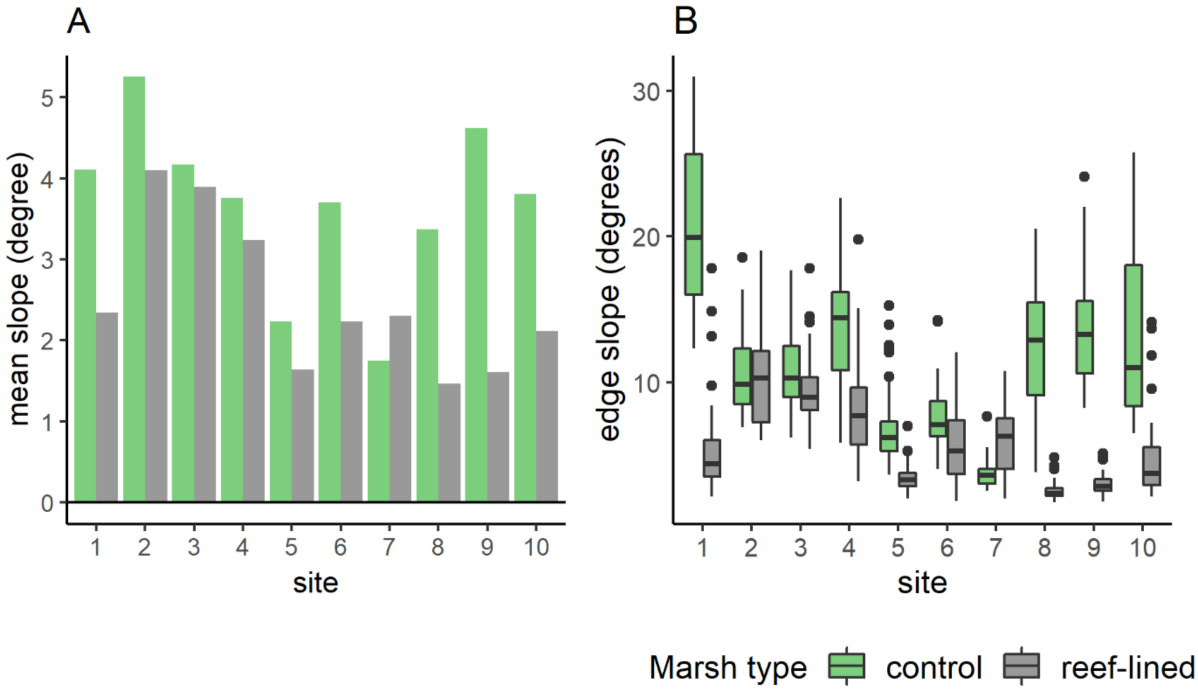

Figure 6. A) Mean buffer area slope and B) edge slope at each site for control and reef-lined marsh edges from transects. Grey bars indicate reef-lined marsh edges and green bars indicate control marsh edges at each site. Components for boxplot are described in the caption for Figure 3.

9. APPENDICES

Table A1. Slope (degree) statistics from buffer areas around marsh edges from Fowling Point Marsh (FP), Chimney Pole Marsh (CP), Matulakin Marsh (MM), and 2 from Hog Island Marsh (HI) surveyed in-situ by McLoughin et al. (2010, 2015).

Site	**In-situ edge classification**	**Min**	**Max**	**Range**	**Mean**	**Std**
CP	Terrace	0.01	29.7	29.6	7.4	5.5
FP	Ramp	0.1	20.9	20.8	4.3	2.8
MM	Scarp	0.1	33.4	33.4	11.0	6.0
HI_terrace	Terrace	0.04	35.9	35.9	5.6	5.9
HI_scarp	Scarp	0.1	40.3	40.2	8.1	9.3

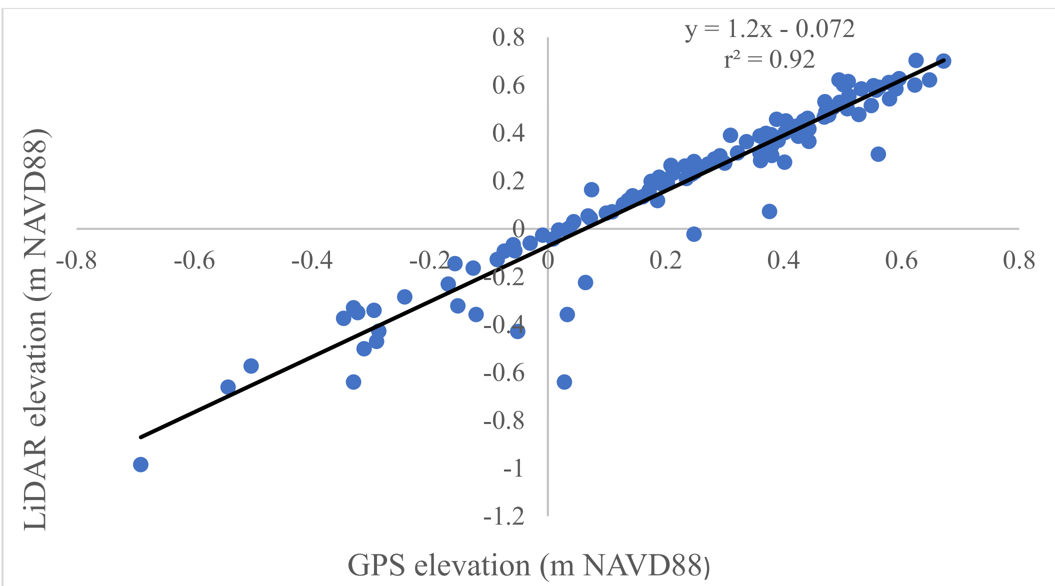

Figure A1. Validation of LiDAR elevation data with in-situ GPS elevations, where LiDAR data was extracted to locations of in-situ data points at Fowling Point Marsh (n = 114).

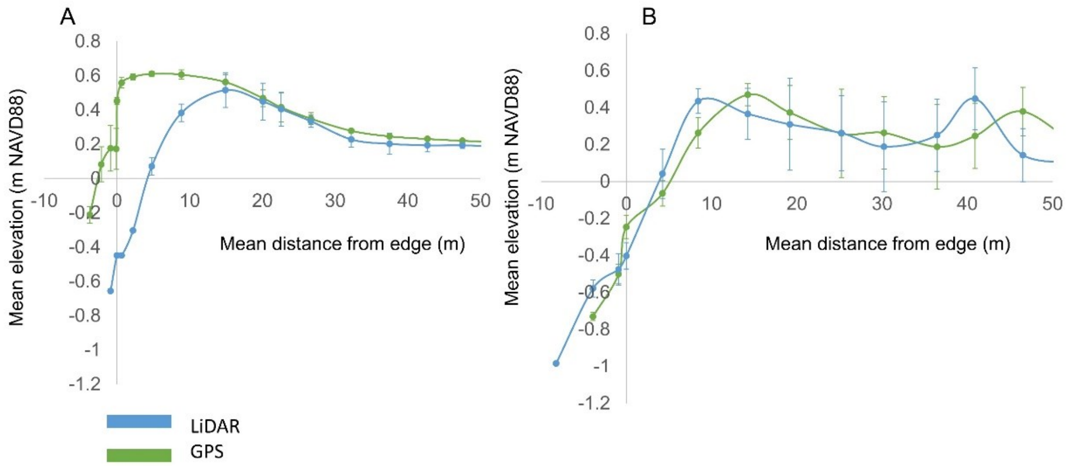

Figure A2. Mean elevation profiles (± standard error from multiple transects) for A) an unstable marsh (CP) showing lateral retreat in the 5 years between surveys and and B) a stable marsh (FP). Distance from the edge is measured on the x-axis, where the edge is at 0 m and positive values are towards the platform.

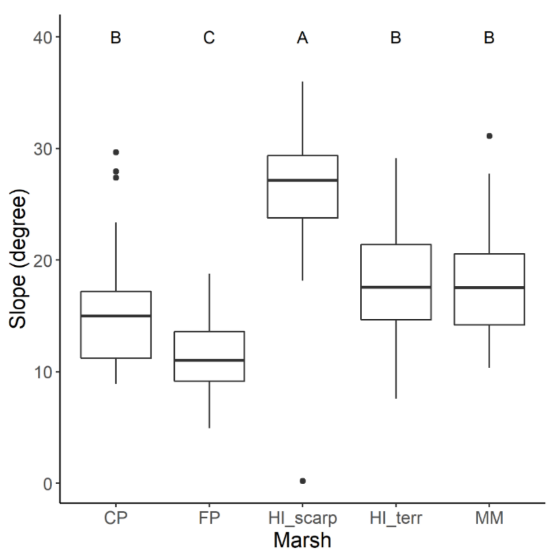

Figure A3. Boxplots of edge slope values found along transects perpendicular to marsh edges. HI scarp had a significantly greater maximum slope than all other marshes, while FP had a maximum that was significantly lower. The maximum slope for CP, HI terrace (HI_terr), and MM, did not significantly differ from one another.